JOURNAL OF MATERIALS SCIENCE 13 (1978) 541–552

Microstructural behaviour and mechanical hardening in a Cu-Ni-Cr alloy

A. CHOU*, A. DATTA†, G. H. MEIER, W. A. SOFFA,
Department of Metallurgical and Materials Engineering, University of Pittsburgh, Pittsburgh, Pennsylvania, USA

In this investigation electron microscopy and diffraction have been employed to characterize the development of the modulated structures and associated sideband phenomena in a Cu–31.6 Ni–1.7 Cr alloy and the microstructural behaviour has been correlated with the age-hardening response. The microstructural behaviour is consistent with the notion of spinodal decomposition of a rather asymmetric alloy within the ternary miscibility gap in the temperature range 650 to 750° C. The modulated structures which form during precipitation tend to undergo a morphological change during subsequent coarsening involving the sequence: cuboids → rods → platelets (or rafts); the driving force for this transformation is the minimization of the surface and strain energy of the coherent two-phase mixtures. Precipitate-free or denuded zones have been observed to develop after prolonged ageing apparently resulting from preferential loss of coherency and coarsening of particles in the vicinity of the grain boundaries. This microstructural heterogeneity gives rise to a "discontinuous coarsening" reaction eventually involving the migration of high-angle boundaries. The mechanical strengthening accompanying the formation of the aligned and periodic precipitate morphologies can be accounted for quantitatively in terms of the interaction of dislocations with the internal stress fields associated with the coherent precipitates.

1. Introduction

Cupronickel alloys are well known for their superior properties in marine service. Substantial strengthening of cupronickels can be achieved through precipitation hardening of these nominally copper–nickel alloys modified by ternary and quarternary additions without significant loss of corrosion resistance and fabricability [1–5]. A series of high-strength Cr-bearing cupronickels has been developed and these alloys have been reported to derive their properties through spinodal decomposition [4, 5].

Phase equilibria in the Cu–Ni–Cr system have been investigated experimentally and theoretically by Meijering, *et al.* [6, 7] who have shown the existence of a stable miscibility gap in the ternary system and on cooling a single f c c phase decomposes into two conjugate f c c phases of slightly different lattice parameters. Fig. 1 shows a calculated and experimental isothermal section of the ternary system at 930° C. The theoretical diagram, calculated using a regular solution model, agrees quite well with the experimental diagram. Manenc [8] first reported the appearance of "sidebands" in X-ray patterns during ageing of Cu–Ni–Cr alloys similar to those observed in the Cu–Ni–Fe system by Bradley [9] and interpreted by Daniel and Lipson [10, 11] in terms of a "wave-like" clustering or periodic redistribution of solute atoms during phase separation. Badia *et al.* [4, 5] verified the occurrence of sideband phenomena and the formation of the so-called modulated structures during ageing within the miscibility gap and concluded that spinodal decomposition

*Present address: Department of Materials Science and Engineering, National Tsing Hua University, Taiwan, ROC.
†Present address: Allegheny Ludlum Steel Corporation Research Center, Brackenridge, Pennsylvania, USA.

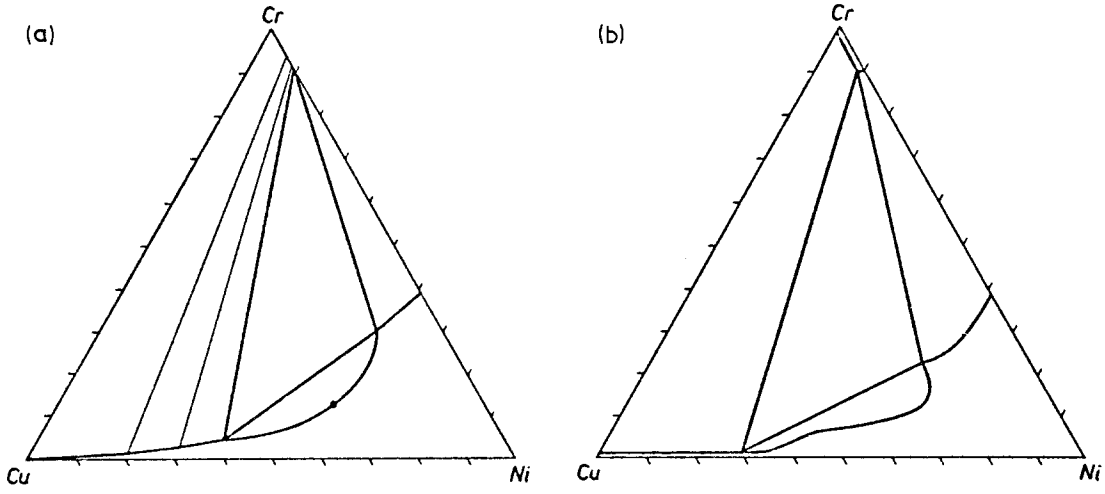

Figure 1 Isothermal section of the Cu–Ni–Cr system at 930° C, (a) calculated, (b) experimental [6, 7].

occurred in the Cr-hardened cupronickels. The preliminary microstructural studies of Mihalisin *et al.* [5] working with a Cu–30 Ni–1.7 Cr alloy and a Cu–28.3 Ni–2.8 Cr alloy and Kreye and Pech [12] working with a Cu–30 Ni–2.9 Cr alloy, indeed, show the formation of modulated structures and sideband phenomena consistent with the notion of spinodal precipitation within the ternary miscibility gap.

Morral and Cahn [13–15] and de Fontaine [16] have extended the treatments of spinodal decomposition in binary systems to consider clustering and ordering in ternary systems. The analysis of the thermodynamic stability of a supersaturated state within a ternary miscibility gap requires that the directional derivative on the free energy surface be considered. The curvature of the free-energy–composition surface is positive in all directions if

$$\frac{\partial^2 F}{\partial x_A^2}\frac{\partial^2 F}{\partial x_B^2} > \left(\frac{\partial^2 F}{\partial x_A \partial x_B}\right)^2$$

and

$$\frac{\partial^2 F}{\partial x_A^2} > 0,$$

where x_A and x_B are the two independent compositional variables and F is, of course, the molar free energy of the ternary solution. When

$$\frac{\partial^2 F}{\partial x_A^2}\frac{\partial^2 F}{\partial x_B^2} < \left(\frac{\partial^2 F}{\partial x_A \partial x_B}\right)^2$$

the free energy surface is saddle-shaped and the curvature is positive or negative, depending on the direction within the Gibbs triangle, and the curvature is negative in all directions when

$$\frac{\partial^2 F}{\partial x_A^2}\frac{\partial^2 F}{\partial x_B^2} > \left(\frac{\partial^2 F}{\partial x_A \partial x_B}\right)^2$$

and

$$\frac{\partial^2 F}{\partial x_A^2} < 0.$$

The chemical spinodal in a ternary system is given by

$$\frac{\partial^2 F}{\partial x_A^2}\frac{\partial^2 F}{\partial x_B^2} - \left(\frac{\partial^2 F}{\partial x_A \partial x_B}\right)^2 = 0$$

defining a curve along which there is just one direction in which the curvature is zero. Meijering [17, 18] has discussed the shapes of a variety of spinodal surfaces in ternary systems along with sections of corresponding phase diagrams. Ternary systems are essentially affected by strain energy in a manner similar to binary systems.

The classical Cu–Ni–Fe ternary alloys which have been thoroughly studied behave as pseudo-binary alloys and precipitation essentially occurs by redistribution of Cu atoms. The Cu–Ni–Cr system represents the more general ternary case.

The development of commercially significant alloys which are apparently strengthened by modulated structures deriving from spinodal decomposition in binary and ternary systems has

served to focus new attention on the origin of mechanical strengthening in spinodal alloys. Schwartz and co-workers [19, 20] have recently provided a critical examination of mechanical strengthening in spinodal alloys or in alloys strengthened by fine-scale, periodic arrays of coherent precipitates. Continued progress in this area will provide a fundamental basis for the exploitation of the full potential of spinodal or modulated structures in alloy design.

In this paper the results of an electron metallographic study of the precipitation reactions occurring in an aged Cu–31.6 Ni–1.7 Cr alloy are reported. Also, the microstructural behaviour has been correlated with the mechanical hardening observed during ageing.

2. Experimental

2.1. Materials and heat treatment

The Cu–Ni–Cr alloy used in this investigation was supplied by the International Nickel Company and the detailed processing schedule has been described elsewhere [4, 5]. The composition is given in Table I.

The alloy was processed to sheet by cold rolling and annealing at 900° C for 3 h and quenched into ice brine. The material was subsequently aged at 650, 700, and 750° C for ageing times ranging from 5 min to 410 h. During all heat treatments, except for the very short ageing times, the specimens were contained in Ti-gettered evacuated quartz capsules and quenched by breaking the capsules in the quenching bath.

2.2. Electron metallography

Thin foils for electron metallography were prepared by electropolishing 3 mm diameter disc specimens punched from heat-treated sheets. Final polishing was accomplished in a twin-jet electropolisher using a solution containing 375 ml acetic acid, 75 g chromium trioxide, 15 ml H_2O, and 125 ml orthophosphoric acid. The foils were examined at 100 kV.

2.3. Mechanical testing

The room temperature tensile properties of specimens aged at 650° C for different times were determined using a standard Instron testing machine. Sheet tensile specimens 0.3 in. wide, 0.015 in. thick with a 1.0 in. gauge length were used. The tensile specimens were carefully electropolished to remove any surface scratches and oxidation products prior to testing. A strain rate of 4×10^{-2} min^{-1} was employed for all tensile tests. The yield stress was defined in terms of the 0.2% offset strain.

TABLE I Composition (wt. %)

Ni	*Cr*	*Fe*	*Mn*	*Zr*	*Cu*
31.6	1.7	0.28	0.03	–	Balance

3. Results

3.1. Microstructural behaviour

In this study, no evidence of precipitation was discernible in as-quenched specimens; decompo-

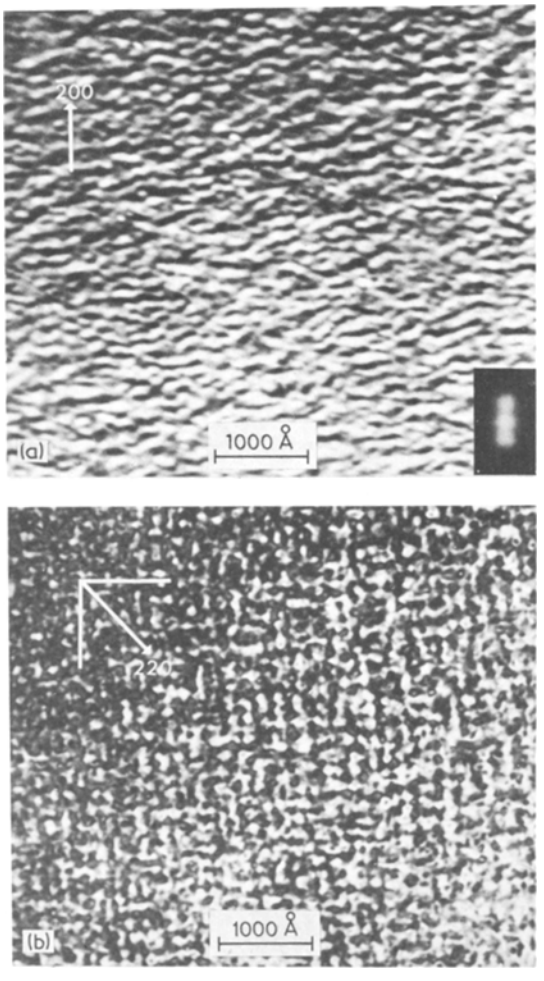

Figure 2 Electron micrographs of Cu–31.6 Ni–1.7 Cr alloy aged at 650° C for 1 h revealing matrix strain contrast striations along traces of the {1 0 0} matrix planes under different imaging conditions; the average wavelength of the modulated structure is ~ 170 Å. (a) Foil normal (0 0 1); g = [$\bar{2}$ 0 0]; insert shows satellite flanking matrix reflection, (b) Foil normal near (0 0 1); g = [2 2 0]; interpenetrating modulations revealed indicative of triaxially modulated structure.

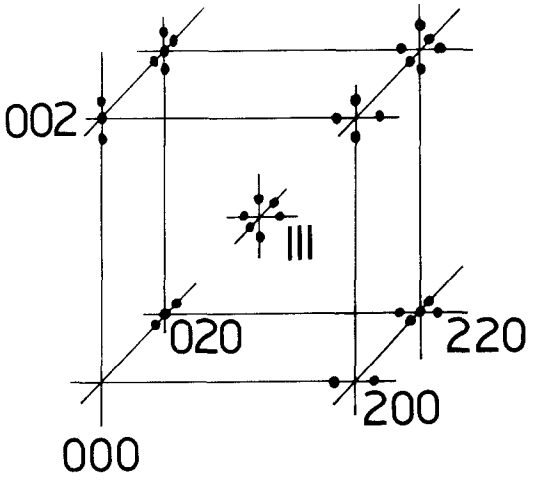

Figure 3 Schematic showing disposition of satellites in reciprocal space.

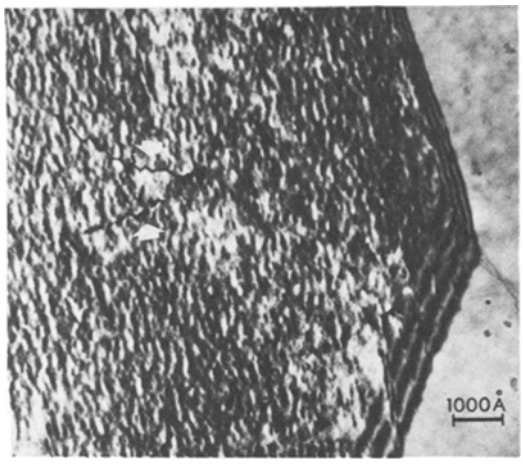

Figure 4 Absence of heterogeneous nucleation on grain boundaries or dislocations clearly reveals the homogeneous nature of the transformation.

sition was apparently suppressed as evidenced by the absence of contrast effects which could be associated with clustering, and selected area diffraction patterns did not exhibit sidebands. After ageing only several minutes to an hour at 650, 700, and 750° C the microstructure was characterized by "wavy" strain contrast striations essentially along the traces of the {1 0 0} matrix planes as shown in Figs. 2a and b. The primary displacement vector **R** characterizing the net matrix strain determined by imaging under different diffracting conditions was found to be principally along ⟨1 0 0⟩. The disposition of satellites in reciprocal space was found to be consistent with the scheme predicted by the simple model of Daniel and Lipson [10, 11] depicted in Fig. 3. The average wavelength, λ, of the triaxially modulated structure can be estimated using a modified Daniel-Lipson relationship for electron diffraction where

$$\lambda = \frac{ha}{(h^2 + k^2 + l^2)} \frac{r}{\Delta r}$$

where r and Δr are the distances from the *hkl* spot to 0 0 0 and "satellite", respectively. Values of the wavelength calculated using this relationship agreed very well with those estimated by direct measurement of the spacing of the strain contrast striations. An important microstructural feature of the initial decomposition process is the absence of preferential precipitation on dislocations and grain boundaries as shown in Fig. 4.

Prolonged ageing gives rise to a periodic array of coherent cuboids with distinct, planar interfaces parallel to the {1 0 0} matrix planes as shown in Fig. 5. During this stage of the precipitation reaction the diffraction spots tend to "split" and show streaking along the ⟨1 0 0⟩ directions indicating the formation of two coherent f c c phases of slightly different lattice parameters. The streaking derives from the coherency strains which induce a local tetragonality in the vicinity of the coherent interphase interfaces [21]. The diffraction contrast exhibited by the coherent cuboidal particles is found to be accurately described by the analysis of Sass *et al.* [22]. Fig. 6 shows that the microstructure resulting from precipitation is still

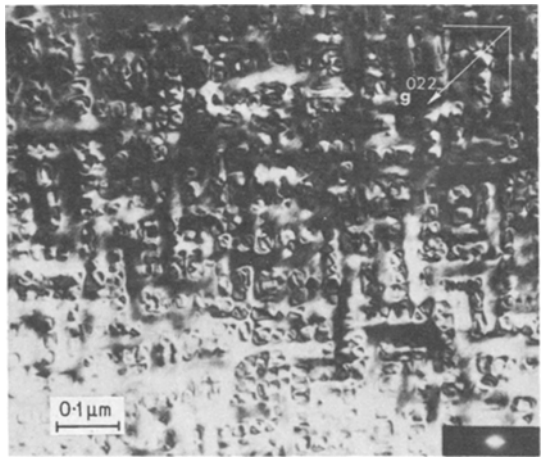

Figure 5 Cu–31.6 Ni–1.7 Cr alloy aged for 24 h at 650° C showing a modulated structure consisting of a periodic array of cuboids with faces essentially parallel to the {1 0 0} matrix planes; insert shows streaking along ⟨1 0 0⟩ deriving from coherency strains.

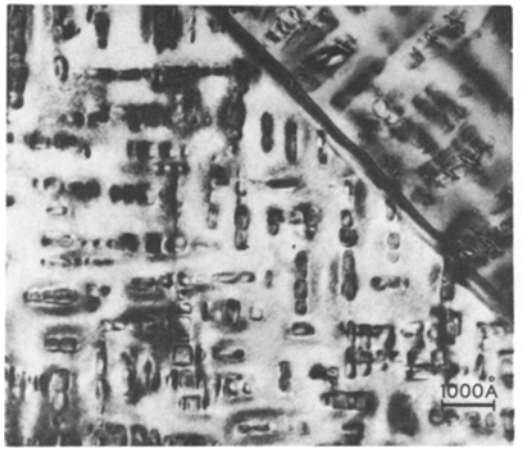

Figure 6 Cu–31.6 Ni–1.7 Cr alloy aged for 25 h at 700° C showing the absence of precipitate-free zones at grain boundaries.

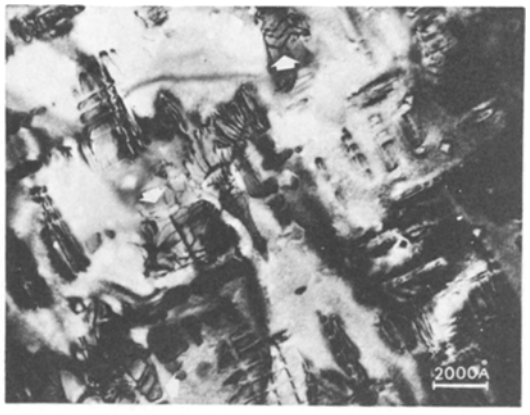

Figure 8 Cu–31.6 Ni–1.7 Cr alloy aged for 200 h at 700° C showing rafts and rods and loss of coherency as evidenced by the development of interfacial dislocations at the interphase interfaces.

relatively uniform and homogeneous right up to the grain boundaries even after the cuboidal precipitate morphology has evolved. At 650° C, maximum strength is obtained when the microstructure consists of a periodic array of cuboids having an average edge width of about 120 Å and the average wavelength, λ, of the periodic and aligned microstructure is approximately 200 Å. The coarsening of the modulated structure at 650, 700, and 750° C obeyed a $\lambda^3 - \lambda_0^3 = Kt$ kinetic law, where λ_0 is the wavelength at the onset of coarsening and t is the ageing time. The experimental activation energy for the coarsening process was found to be approximately 41 kcal mol^{-1}.

Longer ageing times in excess of about 24 h show a change from a periodic three-dimensional array of cuboidal particles towards a rod-like and/or plate-like morphology as the cuboids align in rows or rafts and coalesce. The advanced stages of this morphological transformation are clearly revealed in Figs. 7 and 8. The rod-like morphology which develops by aggregation and coalescence of individual cuboids is clearly revealed by a characteristic elongated strain contrast shown in Fig. 9. During this stage of morphological transformation

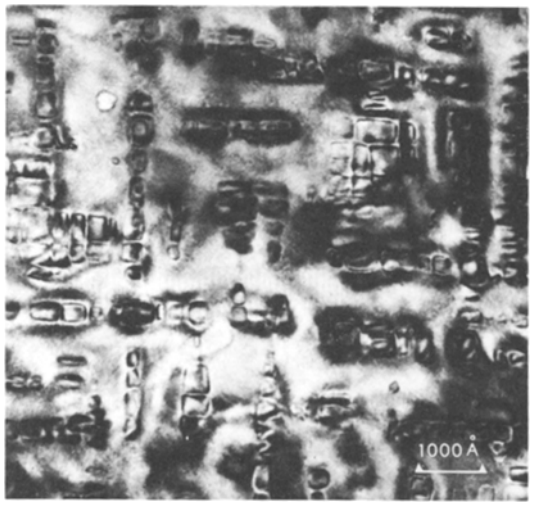

Figure 7 Cu–31.6 Ni–1.7 Cr alloy aged for 200 h at 650° C showing tendency of cuboids to congregate into rafts and rods.

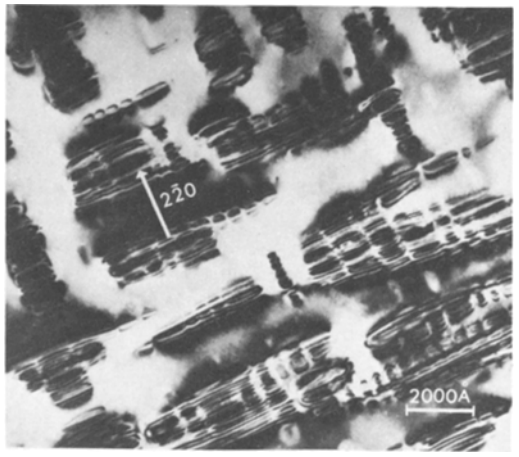

Figure 9 Cu–31.6 Ni–1.7 Cr alloy aged for 200 h at 700° C clearly showing tendency for rod formation as evidenced by characteristic elongated matrix strain contrast.

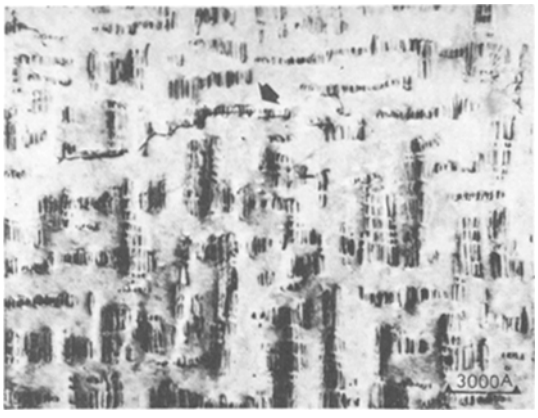

Figure 10 Direct evidence of attraction of matrix dislocations to the coherent interphase interfaces through elastic interaction.

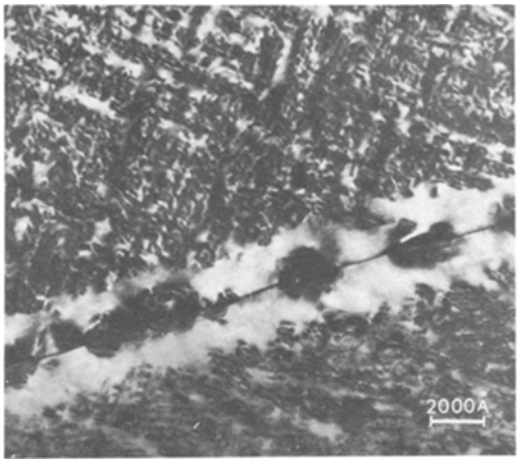

Figure 11 Cu–31.6 Ni–1.7 Cr alloy aged 73 h at 650° C showing the development of precipitate-free or denuded zones in the vicinity of the grain boundaries.

the microstructure becomes somewhat inhomogeneous exhibiting rather large variations in interparticle spacing and particle size. Concurrent with the cuboids → rods → plates transformation loss of coherency occurs as evidenced by the appearance of misfit accommodating interfacial dislocations at the interphase interfaces, as seen in certain regions of Fig. 8. The interfacial dislocations are $a/2\langle 1\,1\,0\rangle$ matrix slip dislocations attracted to the growing particles through elastic interaction with the coherency stress fields. Fig. 10 shows this process occurring in a specimen aged 72 h at 700° C. The rods and plates become semi-coherent by matrix dislocations wrapping around them by complex glide and climb mechanisms.

Another important feature of the microstructural behaviour after very long ageing times is the appearance of precipitate-free or denuded zones in the vicinity of the grain boundaries as the result of a grain boundary reaction, as shown in Fig. 11. These precipitate-free zones apparently derive from a preferential coarsening of particles at or in the vicinity of the grain boundaries. Particles near the grain boundaries appear to lose coherency relatively rapidly, while those particles within the grains remain coherent. Figs. 12 and 13 show the formation of coarse semi-coherent precipitates at a grain boundary and a number of particles in the vicinity of the boundary in the process of capturing dislocations. Fig. 13 reveals the formation of a fairly well-developed misfit dislocation structure at the interface of a large irregular particle in the vicinity of a grain boundary. The hexagonal

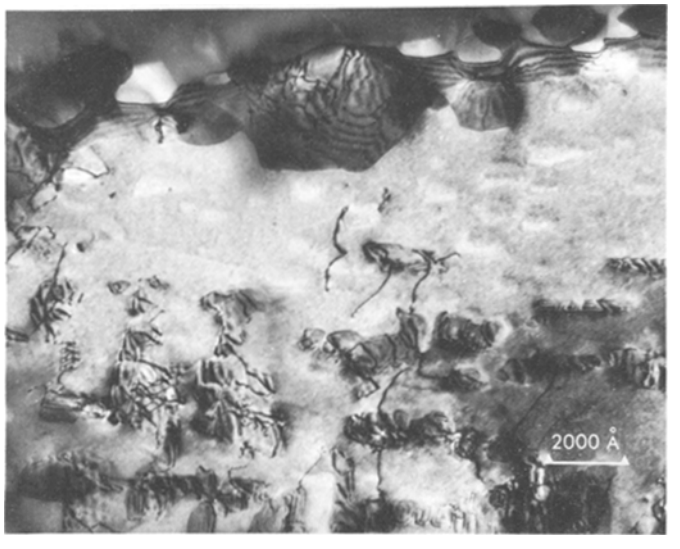

Figure 12 Direct evidence of precipitates in the near vicinity of a grain boundary losing coherency through attraction of matrix dislocations.

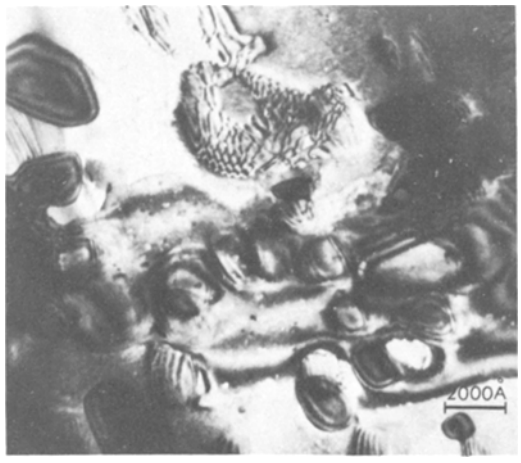

Figure 13 Large semi-coherent particles in the near vicinity of a grain boundary.

array which is forming consists of three sets of dislocations of the type $a/2\langle 1\,1\,0\rangle$.

3.2. Mechanical properties

The results of the yield stress measurements for isothermal ageing at 650° C are shown in Fig. 14. It is evident that the Cu–31.6 Ni–1.7 Cr alloy shows a substantial age hardening response. The yield stress of the as-quenched alloy was ~ 13 kg mm^{-2}. The yield stress increased rapidly during ageing and reached a maximum of ~ 26 kg mm^{-2} after about 2 h at 650° C and then exhibited a rather broad peak during subsequent ageing. The critical resolved shear stress, τ_c, of the age-hardened alloy at peak strength was estimated from the polycrystalline tensile data using a Taylor factor of 3. This analysis yields a value of $\tau_c \sim 8$ to 9 kg mm^{-2}. The increment in the critical resolved shear stress, $\Delta\tau_c$, taken as the measured yield stress minus that observed for the undecomposed alloy, is estimated to be about 4 to 5 kg mm^{-2}.

4. Discussion

4.1. Microstructural behaviour

Transmission electron microscopy and diffraction have revealed microstructural features and diffraction effects during the ageing of the Cu–31.5 Ni–1.7 Cr alloy similar to the results reported in the literature for a number of sideband alloys, including the Cu–Ni–Fe [23–25], Cu–Ti [26–28], Ni–Ti [29, 30], Cu–Ni–Sn [19, 20], and Nb–Zr [31] systems. The electron metallographic observations suggest that the Cu–31.6 Ni–1.7 Cr alloy aged in the range 650 to 750° C decomposes within the ternary miscibility gap through the formation and development of extended compositional fluctuations along the elastically "soft" $\langle 1\,0\,0\rangle$ directions. The attendant sideband effects are consistent with the notion of a "wave-like" clustering or the development of concentration waves along the three mutually orthogonal $\langle 1\,0\,0\rangle$ directions producing a triaxially modulated structure. The compositional modulations are accompanied by periodic variations in the lattice parameter and scattering factor giving rise to the so-called "satellites" or "sidebands" [10, 11, 32, 33]. The initial breakdown of the supersaturated state was found to be relatively structure-insensitive as evidenced by the absence of heterogeneous nucleation at structural singularities such as dislocations and grain boundaries, and the periodicity and alignment characteristic of these fine-scale, periodic coherent precipitate morphologies is evident from the earliest stages of decomposition. It is concluded here that the decomposition of the supersaturated solid solu-

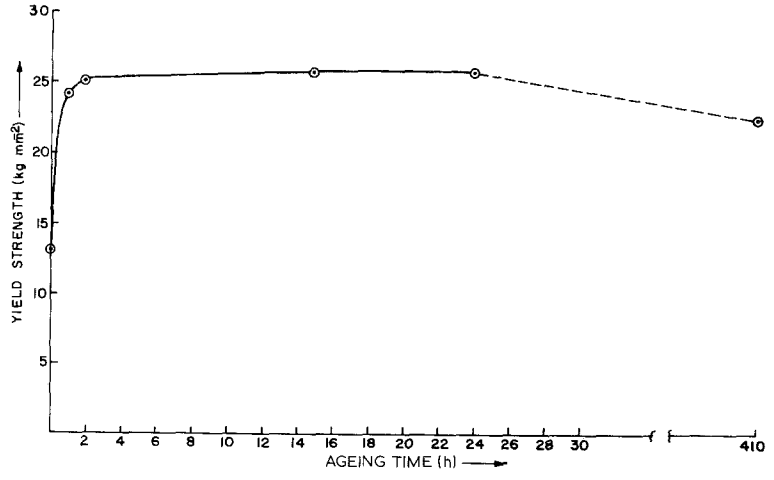

Figure 14 Age-hardening curve of the Cu–31.6 Ni–1.7 Cr alloy aged at 650° C.

tions within the miscibility gap was initiated by spinodal decomposition of a rather asymmetric alloy. Of course, the occurrence of spinodal decomposition cannot be established categorically based solely on microstructural evidence, although the microstructural behaviour and diffraction effects observed in these studies are virtually identical to those observed in alloys known to undergo spinodal decomposition as cited above. However, recent investigators [28, 34–36] have pointed out that aligned and periodic precipitation with accompanying sideband phenomena can derive from elastic interaction during classical nucleation, growth, and/or coarsening in an elastically anisotropic matrix, and the microstructural development is likely to be virtually indistinguishable from spinodal decomposition.

The morphological transformation cuboids → rods → platelets or rafts observed in the Cu–Ni–Cr alloy during prolonged ageing can be understood in terms of the work of Khachaturyan [35, 36] which has shown that a periodic or quasi-periodic coherent two-phase mixture can progressively lower the elastic strain energy of the system by undergoing such a transformation during coarsening. Khachaturyan's analysis shows that the periodic morphology of highest free energy is a three-dimensional array of cuboids. A periodic array of rods has a lower free energy and the lowest free energy morphology consists of a periodic array of platelets. Actually, the three-dimensional arrays of cuboids or rods in this analysis contain some partially decomposed matrix and thus these morphologies actually have higher chemical free energies than the platelet morphology. The morphological transformation is effected during coarsening by stress-affected diffusion [34].

Although no rigorous or comprehensive coarsening theory yet exists describing coarsening of modulated structures, a number of investigators have reported a $\lambda^3 - \lambda_0^3 = Kt$ or $t^{1/3}$ type relation as predicted by the Lifshitz–Slyozov–Wagner (L–S–W) theory [37, 38] of Ostwald ripening which was derived on the basis of volume-diffusion controlled coarsening of a random array of spherical particles driven by the overall decrease in surface energy. The coarsening of coherent precipitates under the apparent mutual influence of elastic strain and surface energy also has been reported to essentially obey the L–S–W theory in a number of Ni-base alloys [34, 39, 40]. A slightly modified L–S–W theory has been developed to describe the coarsening behaviour in Ni–Cr–Al and Ni–Al alloys at large volume fractions [41]. The elastic interaction appears to act only as a perturbation on the coarsening process distorting the diffusion fields, resulting in a selectivity through anisotropic stress-affected diffusion alluded to earlier. However, the coarsening kinetics during the development of extended compositional modulations is not well understood at all, although Cahn [42] has made a preliminary investigation of the latter stages of spinodal decomposition and the beginnings of particle coarsening. Furthermore, some investigators [43] have suggested that a $t^{1/2}$ relation should be expected to describe the volume-diffusion controlled coarsening in a number of modulated alloys considering the spatial distribution and morphology of the particles. It is concluded here that the fundamental basis for $\lambda^3 - \lambda_0^3 = Kt$ or $t^{1/3}$ relationships reported to govern the coarsening behaviour of modulated structures from the very early stages of precipitation is not well understood.

The experimental activation energy of ~41 kcal mol^{-1} for the coarsening reaction in the Cu–Ni–Cr alloy appears rather low; however, this value could reflect an effect of quenched-in vacancies on the diffusion-controlled reaction [44]. The experimental value of 41 kcal mol^{-1} might represent the activation energy for migration of the rate controlling species rather than the activation energy for diffusion which is a composite term including the energy of formation of vacancies in the alloy. Significant scatter was observed in the coarsening data which might be explained by a variable excess vacancy concentration.

The formation of precipitate-free zones (PFZs) has been widely studied in high-strength Al-base alloys and these effects generally have been correlated with vacancy and/or solute depletion in the vicinity of the grain boundaries and the attendant effects on nucleation and growth of zones and metastable or stable precipitates occurring in the precipitation sequence. Importantly, the presence of these "precipitate-free" or "denuded" zones at the grain boundaries is recognized to affect the ultimate properties of age hardened alloys including the ductility, fatigue resistance, and stress-corrosion cracking susceptibility [45–49]. In the age hardened Cu–Ni–Cr alloy studied in this investigation apparent precipitate-free zones

developed at the grain boundaries subsequent to the homogeneous precipitation reaction after prolonged ageing. This microstructural heterogeneity is characterized by large semicoherent particles at or in the vicinity of the grain boundaries surrounded by large denuded regions as shown in Figs. 11, 12, and 13. The particles near the grain boundaries lose coherency more rapidly since the boundary can provide a supply of misfit accommodating dislocations which are attracted to the precipitate/matrix interfaces through elastic interaction with the coherency strain fields. The transformation from a state of coherency to semi-coherency for particles within the grain depends on the availability of matrix dislocations. The semi-coherent grain boundary particles grow or coarsen at the expense of the coherent phase mixture within the grains. Short circuit diffusion along the grain boundary can also provide for preferential coarsening of the grain boundary particles. The denuded region grows out behind a reaction front across which there is a relaxation of surface and strain energy, and the process might be called a "discontinuous coarsening" reaction [50–52] initiated by morphological heterogeneities deriving primarily from the unequal rates of loss of coherency and coarsening. After longer ageing times the discontinuous coarsening reaction involves the migration of segments of certain grain boundaries similar to cellular or discontinuous precipitation as discussed by Gronsky and Thomas [51] in their studies of spinodally decomposed Cu–Ni–Fe alloys. The migrating grain boundary moves up to the reaction front and the coarse arrays of irregularly shaped semi-coherent particles grow into the grains behind the sluggishly-moving boundary with the coarsening reaction occurring at the front via grain boundary diffusion. The reduction in total interfacial free energy and strain energy provides the driving force for the migration of the grain boundary into the predominantly coherent, two-phase mixture within the grains. However, initial migration of the boundaries subsequent to the formation of the coarse grain boundary precipitates and denuded regions, is perhaps triggered by normal grain growth tendencies or boundary curvature as proposed by Fournelle and Clark [53] in their discussion of the genesis of cellular colonies in discontinuous precipitation. The latter aspects of the grain boundary reaction will be described and discussed in a subsequent paper.

4.2. Mechanical hardening

Although the yield stress measurements were defined in terms of 0.2% offset strain and, therefore, subject to the effects of work hardening during the early stages of yielding, some interesting and important results stem from a quantitative analysis of the origin of the observed strengthening.

Cahn [54] has analysed the interaction of dislocations with a periodically varying internal stress field resulting from spinodal decomposition; however, the analysis is essentially applicable as a first approximation to the interaction of slip dislocations with a macrolattice of periodically varying obstacles regardless of the origin of the modulated structure. Cahn's internal strain hardening model incorporates analogues of both the Mott and Nabarro theory [55] and classical Orowan mechanism [56]. The model identifies two domains defined by extreme values of the parameter $A\eta Y\mathbf{b}/\gamma\beta$ where

A = amplitude of the composition fluctuations or modulations

η = distortion parameter = $\dfrac{\partial \ln a}{\partial c}$

Y = Young's modulus

$\mathbf{b}$ = Burgers vector

γ = line tension of the dislocations

β = wave vector = $2\pi/\lambda$;

λ is the wavelength of the modulated structure. For $A\eta Y\mathbf{b}/\gamma\beta < 1$, there is little bending or bowing of the mobile dislocations and the critical resolved shear stress required to move the essentially straight dislocations through the periodically varying stress field is given by;

$$\tau_0^{\mathrm{s}} = \frac{A^2\eta^2 Y^2\mathbf{b}}{3\sqrt{6}\beta\gamma} \quad \text{(for screws)}$$

$$\tau_0^{\mathrm{e}} = \frac{A^2\eta^2 Y^2\mathbf{b}}{\sqrt{2}\beta\gamma} \quad \text{(for edges).}$$

The barrier to edge dislocation motion is about 5 times that encountered by screw components. For $A\eta Y\mathbf{b}/\gamma\beta > 1$, the dislocations bow or bend around the particles (analogous to the Orowan bypass mechanism) and the critical resolved shear stress is given by;

$$\tau_0 = 0.57(A\eta Y)^{1/3}\left(\frac{\gamma\beta}{b}\right)^{2/3}$$

in this formulation. Therefore, Cahn's internal strain hardening model predicts a rising portion of the ageing curve proportional to λ, the wavelength of the modulated structure, and a branch which falls off as $\lambda^{-2/3}$. The rising branch is the analogue or modification of the Mott and Nabarro theory [55] and the falling branch is the analogue of Orowan hardening [56].

The hardening by the modulated structure in the Cu–Ni–Cr alloy falls well within the first domain. If the critical stress estimated by Cahn, τ_0, is identified with the increment in the critical resolved shear stress, $\Delta\tau_c$, resulting from precipitation hardening, using the elastic constants of pure Cu [57] and the data of Badia *et al.* [5] and Meijering *et al.* [6] a value of ~ 2 to $10\,\mathrm{kg\,mm^{-2}}$ is predicted compared with an observed value of 4 to $5\,\mathrm{kg\,mm^{-2}}$. The upper limit predicted by Cahn's theory is the critical stress for edge mobility and the lower limit for screw dislocation mobility. Considering that the experimental values of the critical resolved shear stress are probably overestimates by as much as 20% because of the effects of work hardening, and that perhaps the macroscopic yielding behaviour will generally derive from some average behaviour of the edge and screw components within the dislocation arrays, it is concluded here that Cahn's theory of spinodal hardening predicts at least the magnitude of the observed strengthening in the Cu–31.6 Ni–1.7 Cr alloy hardened by modulated structures to within a factor of 2 or better.

Schwartz and co-workers [19, 20] have recently examined the mechanical strength of spinodal alloys or alloys strengthened by modulated structures. In their analysis it is concluded that the Cu–31.6 Ni–1.7 Cr alloy offers no comparison with Cahn's theory based essentially on the preliminary results of Badia *et al.* [4, 5] and further concluded that the yield stress theory of Gerold and Haberkorn [58] best fits the experimental data. The Gerold and Haberkorn version of the critical stress is;

$$\tau_0 = \alpha G(\epsilon)^{2/3}\left(\frac{R}{b}\right)^{1/2} f^{1/2}$$

where $\alpha = 1$ for screws and 3 for edges

G = matrix shear modulus

ϵ = linear matrix/particle misfit, $\frac{\Delta a}{a}$

R = particle radius

f = volume fraction.

The microstructure at maximum strength in the Cu–Ni–Cr alloy consists of a periodic array of cuboids aligned along the $\langle 1\,0\,0\rangle$ matrix directions with faces essentially parallel to the $\{1\,0\,0\}$ matrix planes. Taking $(D/\lambda)^3 = f$, where D is the average length of a cube edge and $2R \approx D$; $\epsilon = \Delta a/a \sim 0.6 \times 10^{-2}$, $\lambda \sim 200$ Å, $R \sim 60$ Å, and using the elastic constants of pure copper yields a calculated value of the critical stress of ~ 7 to $21\,\mathrm{kg\,mm^{-2}}$. The lower limit for screw mobility does indeed agree rather well with the experimentally observed values.

Schwartz and co-workers [19, 20] have pointed out that Cahn's model should be somewhat of an underestimate of the strengthening since the analysis is strictly applicable to the early stages of ageing when a sinusoidal profile is approximated; however, the modulated structure that evolves after longer ageing times is best described by a square or rectangular wave form and the strengthening should, in general, derive for a summation over a spectrum of wavelengths. The results obtained in this study suggest that a modification of Cahn's analysis to include the effects of a generalized composition profile should provide excellent agreement with the experimental results. However, the lower bound of the Gerold and Haberkorn theory based on the interaction of screw dislocations with the short range coherency stress fields of the particles also predicts the strengthening to certainly within a factor of 2 or better. Importantly, as the modulated structure evolves towards a square or rectangular wave form and as the interfaces sharpen, the coherency stresses become more localized at the discrete interphase interfaces. Cahn's theory may describe accurately the early stages of hardening and a generalization of the Cahn treatment may converge to the Gerold and Haberkorn model as the interfaces sharpen and discrete particles evolve.

The analysis presented here certainly is not a critical evaluation of the strengthening models discussed since a rigorous correlation between the experimental results and predicted hardening behaviour would require correlation between not only the levels of strengthening but also between

the variation of the yield strength with salient microstructural parameters such as the wavelength, particle size, volume fraction, etc. However, the attempt presented here to establish an approximate quantitative relationship between microstructure and properties in these age-hardened alloys suggests that one can conclude that the mechanical strengthening deriving from the formation of the modulated structures in the Cu–31.6 Ni–1.7 Cr alloy can be accounted for quantitatively in terms of the interaction of dislocations with the internal stress fields associated with the coherent precipitates.

5. Conclusions

(1) Transmission electron microscopy and diffraction have revealed the formation of modulated microstructures and associated sideband phenomena in a Cu–31.6 Ni–1.7 Cr alloy aged within a ternary miscibility gap in the temperature range 650 to 750° C, and the microstructural behaviour is consistent with the notion of spinodal decomposition of a rather asymmetric alloy.

(2) The modulated structures which develop tend to undergo a morphological change during coarsening involving the sequence: cuboids → rods → platelets (or rafts); and the driving force for this transformation is the minimization of the surface and strain energy of the coherent two-phase mixtures.

(3) Precipitate-free or denuded zones tend to develop after long ageing times, and this microstructural heterogeneity appears to derive primarily from a relatively rapid loss of coherency of precipitate particles at or near the grain boundaries, and the preferential growth or coarsening of these particles at the expense of the coherent particles within the grains. The particles within the grains lose coherency predominantly by the attraction and adsorption of matrix dislocations, whereas the grain boundaries apparently can readily supply misfit dislocations to particles near grain boundaries.

(4) The coarse precipitate structure and denuded regions in the vicinity of the grain boundaries trigger the migration of certain boundaries and the "discontinuous coarsening" reaction eventually involves the migration of high-angle grain boundaries and boundary diffusion, analogous to cellular or discontinuous precipitation.

(5) The mechanical strengthening deriving from the formation of modulated structures in the Cu–31.6 Ni–1.7 Cr alloy can be accounted for quantitatively in terms of the interaction of dislocations with the internal stress fields associated with the coherent precipitates.

Acknowledgements

This work was supported in part by the National Science Foundation under grant No. DNR73-02436 A01. Also, this work was done in partial fulfilment of the requirements for the Master of Science degree in the Department of Metallurgical and Materials Engineering at the University of Pittsburgh by one of the authors (AC).

References

1. J. N. BRADLEY, *Inst. Met. Rev.* **17** (1972) 81.
2. S. P. GUPTA, A. A. JOHNSON and K. MUKHERJEE, *Mater. Sci. Eng.* **9** (1972) 97.
3. S. P. GUPTA and K. MUKHERJEE, *ibid* **10** (1972) 43.
4. F. A. BADIA, G. N. KIRBY and J. K. MIHALISIN, *ASM Transactions Quarterly* **60** (1967) 395.
5. J. R. MIHALISIN, E. L. HUSTON and F. A. BADIA, Second International Conference on the Strength of Metals, Vol. II, (ASM, 1970) p. 679.
6. J. L. MEIJERING, G. W. RATHENAU, M. G. STEEG and B. BRAUN, *J. Inst. Metals* **84** (1955) 118.
7. J. L. MEIJERING, *Acta Met.* **5** (1957) 257.
8. J. MANENC, *ibid* **6** (1958) 145.
9. A. J. BRADLEY, *Proc. Phys. Soc.* **52** (1940) 80.
10. V. DANIEL and H. LIPSON, *Proc. Roy. Soc.* **A181** (1943) 368.
11. *Idem, ibid* **A182** (1944) 378.
12. H. KREYE and P. PECH, *Z. Metallkde* **64** (1973) 765.
13. J. E. MORRAL and J. W. CAHN, *Acta Met.* **19** (1971) 1037.
14. J. E. MORRAL, *ibid* **20** (1972) 1061.
15. *Idem, ibid* **20** (1972) 1069.
16. D. DE FONTAINE, *J. Phys. Chem. Solids* **33** (1972) 297.
17. J. L. MEIJERING, *Phillips Res. Rep.* **5** (1950) 333.
18. *Idem, ibid* **6** (1951) 183.
19. L. H. SCHWARTZ, S. MAHAJAN and J. T. PLEWES, *Acta Met.* **22** (1974) 601.
20. L. H. SCHWARTZ and J. T. PLEWES, *ibid* **22** (1974) 911.
21. A. ARDELL, *Phil. Mag.* **16** (1967) 147.
22. S. L. SASS, T. MURA and J. B. COHEN, *ibid* **16** (1967) 679.
23. R. CADORET and P. DELAVIGNETTE, *Phys. Status Solidi* **32** (1969) 853.
24. E. P. BUTLER and G. THOMAS, *Acta Met.* **18** (1970) 347.
25. R. J. LIVAK and G. THOMAS, *ibid* **19** (1971) 497.
26. T. HAKKARAINEN, Ph.D. Thesis, Helsinki University of Technology, Helsinki (1971).

27. D. E. LAUGHLIN and J. W. CAHN, *Acta Met.* **23** (1975) 329.
28. A. DATTA and W. A. SOFFA, *ibid* **24** (1976) 987.
29. S. L. SASS and J. B. COHEN, *Trans. TMS-AIME* **242** (1968) 1764.
30. K. SAITO and R. WATANABE, *Nat. Res. Inst. Metals* **11** (1969) 153.
31. P. E. J. FLEWITT, *Acta Met.* **22** (1974) 47.
32. M. E. HARGREAVES, *Acta Cryst.* **4** (1951) 301.
33. D. DE FONTAINE, "Local Atomic Arrangements Studied by X-ray Diffraction," edited by J. B. Cohen and J. E. Hilliard, (Gordon and Breach, New York, 1966) p. 51.
34. A. J. ARDELL and R. B. NICHOLSON, *Acta Met.* **14** (1966) 1295.
35. A. G. KHACHATURYAN, *Phys. Status Solidi* **35** (1969) 119.
36. A. G. KHACHATURYAN, *IEEE Trans. Magnetics* **6** (1970) 233.
37. I. M. LIFSHITZ and V. V. SLYOZOV, *J. Phys. Chem. Solids* **19** (1961) 35.
38. C. WAGNER, *Z. Electrochem.* **65** (1961) 581.
39. A. J. ARDELL, *Met. Trans.* **1** (1970) 525.
40. P. K. RASTOGI and A. J. ARDELL, *Acta Met.* **19** (1971) 321.
41. D. J. CHELLMAN and A. J. ARDELL, *ibid* **22** (1974) 577.
42. J. W. CAHN, "The Mechanism of Phase Transformations in Crystalline Solids," (Institute of Metals, London, 1969) p. 1.
43. J. HIGGINS, R. B. NICHOLSON and P.WILKES, *Acta Met.* **22** (1974) 201.
44. T. H. DEKEIJSER, *Scripta Met.* **9** (1975) 193.
45. G. W. LORIMER and R. B. NICHOLSON, *Acta Met.* **14** (1966) 1009.
46. R. B. NICHOLSON, *J. Inst. Metals* **95** (1967) 91.
47. D. W. PASHLEY, M. H. JACOBS and J. T. VIETZ, *Phil. Mag.* **16** (1967) 51.
48. M. H. JACOBS and D. W. PASHLEY, "The Mechanism of Phase Transformations in Crystalline Solids," (Institute of Metals, 1969) p. 43.
49. E. A. STARKE, *J. Metals* **22** (1970) 54.
50. J. D. LIVINGTON and J. W. CAHN, *Acta Met.* **22** (1974) 495.
51. R. GRONSKY and G. THOMAS, *ibid* **23** (1975) 1163.
52. D. B. WILLIANS and J. W. EDINGTON, *ibid* **24** (1976) 323.
53. R. FOURNELLE and J. B. CLARK, *Met. Trans.* **3** (1972) 2757.
54. J. W. CAHN, *Acta Met.* **11** (1963) 1275.
55. N. F. MOTT and F. R. N. NABARRO, *Proc. Phys. Soc.* **52** (1940) 86.
56. E. OROWAN, "Symposium on Internal Stresses in Metals and Alloys," (Institute of Metals, 1948) p. 451.
57. A. KELLY and G. W. GROVES, "Crystallography and Crystal Defects," (Addison-Wesley, Reading, Mass., 1970) p. 163.
58. V. GEROLD and H. HABERKORN, *Phys. Status Solidi* **16** (1966) 675.

Received 11 May and accepted 5 July 1977.